# Snow Albedo Determination Using the NASA MODIS Instrument

A.G. KLEIN[1] AND D.K. HALL[2]

## ABSTRACT

The Moderate Resolution Imaging Spectroradiometer (MODIS) is scheduled for launch aboard the first NASA Earth Observing System platform (Terra-1). MODIS will provide a global daily view of the Earth's seasonally snow-covered areas and daily snow-cover maps will be produced from MODIS data. A prototype algorithm is now being developed to calculate the albedo of these snow-covered surfaces using the seven MODIS visible to short-wave infrared channels designed for land surface studies. The prototype algorithm utilizes a model of the bidirectional reflectance distribution function (BRDF) of snow in calculating the surface albedo. Over forests a simple isotropic scattering model is used while a BRDF model that accounts for the strongly forward scattering nature of snow is employed for non-forested areas including cropland, tundra and ice sheets. Topographic effects are also considered and the spectral albedos from the seven individual MODIS channels will be combined to produce broadband albedos.

Key words: snow albedo, remote sensing.

## INTRODUCTION

Short-wave radiation provides a major energy source for the melting of snow and ice, therefore accurate estimates of the extent of snow and sea ice and the albedo of these surfaces are vital inputs into snowmelt and sea ice models. Compared to other surfaces, both snow and sea ice are highly reflective and their albedo strongly influences surface energy fluxes. Their high albedo strongly influences the Earth's radiation budget (Foster and Chang, 1993) making adequate knowledge of snow and sea-ice extent important inputs into global climate models and surface-atmosphere transfer schemes. In addition to having one of the highest albedos of all naturally-occurring surfaces, the albedo of snow-covered surfaces varies considerably over relatively short time periods. Sea ice can be expected to change on similar or shorter time-scales. To adequately capture the temporal changes in these high albedo surfaces, frequent temporal sampling, preferably daily, is required.

Satellite observations are the most efficient means of documenting the albedo of both snow and sea ice over large areas. The Moderate Resolution Imaging Spectroradiometer (MODIS) is especially well suited for this task as it will image mid-to-high latitude snow-covered areas on a daily basis. Compared with currently operational polar orbiting environmental satellites, MODIS offers cloud detection, higher spatial and finer spectral resolution.

A preliminary prototype of the MODIS snow albedo algorithm is outlined here. Algorithm development has been aided greatly by a number of recently developed algorithms that estimate the albedo of both snow (Knap, 1997; Knap and Oerlemans, 1996; Stroeve *et al.*, 1997) and sea ice (De Abreau *et al.*, 1994; Schweiger *et al.*, 1993). This previous research, particularly

[1] Department of Geography, Texas A&M University, College Station, Texas 77843-3147, U.S.A.
[2] Hydrological Sciences Branch, NASA/Goddard Space Flight Center, Greenbelt, Maryland 20771, U.S.A.

that which has focused on the development of albedo algorithms for the Advanced Very High Resolution Radiometer (AVHRR) instrument, forms a solid basis for the construction of a similar algorithm for MODIS. These approaches are being adapted for use with the MODIS instrument with the goal of designing a state-of-the-art, yet readily comprehensible, algorithm capable of producing an albedo estimate from a single MODIS observation.

## THE MODIS AND MODIS AIRBORNE SIMULATOR (MAS) INSTRUMENTS

MODIS is an imaging radiometer with 36 spectral bands in the visible, reflective-infrared and thermal-infrared wavelengths (0.4 to 14.0 $\mu$m). It is designed to provide key measurements of the land surface, ocean and atmosphere at regional to global scales on a daily basis. Most seasonally snow-covered areas will be imaged daily (Hall *et al.*, 1995). While MODIS has 36 spectral bands, only seven are designed for land surface remote sensing with the spectral and spatial characteristics suitable for use in a MODIS snow albedo algorithm (**Figure 1**). The spatial resolution of these seven MODIS varies from 250 m to 500 m. The spatial resolution of bands 1 and 2 is 250 m, while the spatial resolution of MODIS Bands 3 through 7 is 500 m.

Because MODIS has yet to be launched, the development of the snow albedo algorithm uses data collected by the MODIS Airborne Simulator (MAS). The MAS is an airborne scanning spectroradiometer flown aboard a NASA ER-2 high-altitude research aircraft. At a nominal flight altitude of 20 km, the MAS achieves a spatial resolution of 50 meters. As currently configured, MAS acquires data in 50 spectral channels and approximates most of the MODIS land surface bands (**Figure 1**). Because during imaging, the MAS scans up to ± 45° from nadir, the MAS also simulates the viewing geometry of the MODIS instrument. This similarity is important in the developing a snow albedo algorithm because the measured reflectance from snow or sea-ice surfaces is dependent on the zenith angle and azimuth of the solar beam as well as on the zenith angle and azimuth between the sensor and the ground.

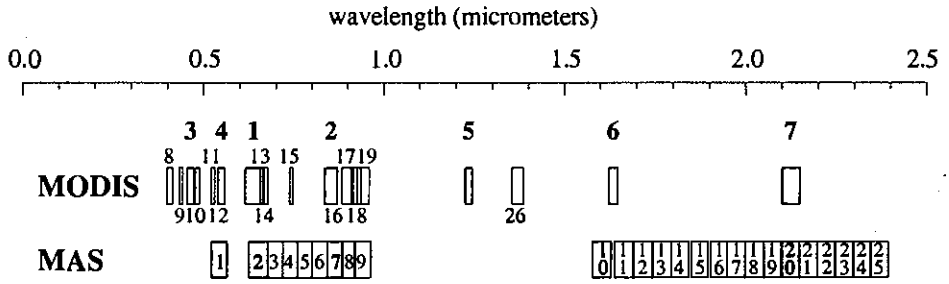


Figure 1: MODIS and MAS bandpasses. The bands used in this study are highlighted in gray.

## STUDY SITE

MAS data collected over central NY State near the city of Oneonta on February 9, 1997 as part of the WINter Cloud Experiment (WINCE) have been used in the initial algorithm prototyping efforts. The moderate relief of the region's glaciated valley and ridge topography enables adequate testing of the topographic correction portion of the algorithm. Ground observations indicate that clear sky conditions prevailed over the area and with the exception of some urban areas and roads, the area was 100% snow-covered at the time of image acquisition. MAS data collected over Madison, Wisconsin, and near Mono Lake, California, will be used to refine the algorithm in the near future.

## THEORETICAL BACKGROUND

Albedo ($\alpha$) is the dimensionless ratio of reflected to incident irradiance measured in a surface-parallel plane:

$$\alpha = \frac{I_r}{I_i} \qquad (1)$$

In-situ measurement of albedo is usually accomplished through the use of two radiometers possessing hemispherical field of views (pyranometers). One pyranometer measures the incident and the other the reflected flux and albedo is calculated by ratioing these fluxes.

This approach to in-situ measurement of albedo has several characteristics that cannot be replicated by a MODIS satellite observation. Adjustments must be made to the radiance received at the sensor to provide accurate albedo estimates. First, the radiance received at the MODIS instrument is not only a function of the physical properties of the snow and the solar and satellite viewing geometries, but also of the state of the atmosphere at the time of image acquisition. Without any changes in the physical properties of the snow-pack, the measured albedo will vary as atmospheric composition changes.

For MODIS, correction for atmospheric effects will be accomplished by using the surface reflectances (MOD 09 product) provided by the MODIS atmospheric correction algorithm (Vermote and Vermeulen, 1999) as opposed to the at-satellite radiances used in the MODIS snow-cover products. In the algorithm prototyping efforts, the 6S atmospheric correction algorithm (Vermote *et al.*, 1997) is being used as a surrogate for the MODIS atmospheric correction algorithm. A detailed description of the potential problems with the MODIS atmospheric correction over snow and ice is beyond the scope of this paper. However, atmospheric corrections over snow will remain a challenge and uncertainties in the effect of aerosols are expected to introduce an uncertainty in snow-albedo calculation of approximately 3% (Yoram Kaufman, personal communication).

A second issue is that the albedo required for energy balance calculations is a *spectrally integrated* quantity. Equation (1) can be rewritten to explicitly express the spectral integration.

$$\bar{a}_s(\theta_0) = \frac{\int a_s(\theta_0,\lambda) F\downarrow(0,\lambda) d\lambda}{F\downarrow(0,\lambda) d\lambda} \qquad (2)$$

Where $F\downarrow(0,\lambda)$ is the spectral incident solar radiation at the snow surface.

However, for land surfaces MODIS only measures radiance in seven relatively narrow bands (**Figure 1**). Converting these spectral albedos ($\alpha_s$) to one or more broadband albedo requires a narrow-to-broadband conversion. The approach employed in the MODIS snow-albedo prototype algorithms is to use a series of weighting coefficients to convert MODIS spectral reflectances to broadband albedos in the visible (0.4-0.7 μm), near-IR (0.7-5.0 μm), and shortwave (0.4-5.0 μm) wavelengths. A set of coefficients specific to MODIS have been recently developed by Liang (1998). However, because the MAS bands differ from MODIS similar coefficients for use with MAS are currently under development. The problem of narrow-to-broadband albedo can be mitigated somewhat by providing both the broadband and spectral albedos, allowing individuals to perform their own narrow-to-broadband conversion if desired.

A third and more pressing problem in estimating albedo from a MODIS satellite observation arises because unlike a pyranometer that provides an integrated measurement of the energy received over an entire hemisphere, the MODIS sensor has a restricted field-of-view. Thus MODIS senses only a small portion of the total energy reflected from the surface.

Like most natural surfaces snow and sea ice are not lambertian reflectors. They do not reflect incident energy uniformly in all directions. Instead the distribution of the reflected energy is unevenly distributed among reflectance angles. Thus, the radiance received at the sensor from a snow-covered surface is strongly dependent on the solar and satellite viewing geometry at the time of image acquisition. As the relationship between the sensor and the sun changes the radiance received at the MODIS sensor from a snow covered surface will vary even if the albedo remains constant.

The angular distribution of the reflected energy is termed the bidirectional reflectance distribution function (BRDF). Following the terminology of Warren (1982), the BRDF is referred to here as R and has the units [$sr^{-1}$]. **Figure 2** illustrates the geometry of the situation:

$$R(\theta_0,\theta',\phi_0,\theta',\lambda) = \frac{dI(\theta',\theta',\lambda)}{\mu_o dF(\theta_0,\phi_0,\lambda)} \qquad (3)$$

Where $\theta_0$ and $\phi_0$ are the incident zenith and azimuth, $\theta'$ and $\phi'$ are the reflection zenith and azimuth, $\lambda$ represents the wavelength dependence, and $\mu_0 = \cos(\theta_0)$. F is the incident flux (taken on a surface normal to the beam) and $I$ is the intensity of the reflected radiation. The initial prototype algorithm assumes that snow and sea-ice surfaces lack azimuthally-oriented structures. This simplifying assumption reduces the azimuthal dependence of R on both $\phi_0$ and $\phi'$ to their relative azimuth ($\phi_0$-$\phi'$). Sastrugi would be an important exception to this simplification.

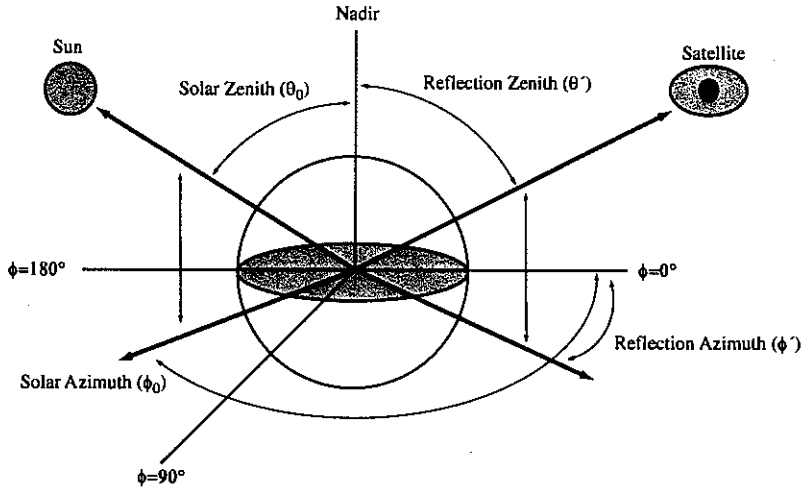


Figure 2: Illustration of the bidirectional reflectance distribution function terminology. After Steffen (1996)

Snow and ice are strongly forward-scattering media. Energy incident upon a snow or ice surface is preferentially reflected in the forward direction. The amount of energy received at the satellite from a snow-covered surface increases as the relative azimuth between the sensor and the sun increases. Failure to account for the forward scattering nature of snow can lead to large errors in albedo determination. As will be illustrated later, the forward scattering becomes more pronounced as the solar zenith angle increases, as grain size increases, and is a greater problem at longer MODIS wavelengths.

In snow and sea-ice albedo algorithms, correction of the radiance received at the sensor for BRDF effects has usually been accomplished by normalizing the BRDF by the albedo to determine an *anisotropic response function* ($f$):

$$f(\theta_0,\theta',\phi_0-\phi',\lambda)=\frac{\pi R(\theta_0,\theta',\phi_0-\phi',\lambda)}{a_s(\theta_0,\lambda)} \qquad (4)$$

Values of $f > 1$ indicate that the reflectance observed at a particular combination of solar zenith angle, sensor zenith angle and relative azimuth is greater than the true spectral albedo at that wavelength while values of $f < 1$ indicated the observed reflectance is less than the true spectral albedo. In order to derive a spectral albedo measurement from a satellite-derived measurement of $R(\theta_0,\theta',\phi_0-\phi',\lambda)$ it is necessary to know the complete distribution of $f(\theta_0,\theta',\phi_0-\phi',\lambda)$ over all combinations of $\theta_0$, $\theta'$ and $\phi_0-\phi'$. As is discussed below, recent advances in the modeling of snow BRFD enable the forward-scattering nature of snow albedo to be taken into account in determining snow and sea-ice albedo from MODIS.

## PRELIMINARY PROTOTYPING EFFORTS

Taking into account the theoretical considerations described above, a preliminary prototype of the MODIS snow-albedo algorithm has been developed. The algorithm uses MAS data collected over central New York on February 9th, 1997 to simulate the MODIS instrument (**Figure 3**). Unlike the MODIS snow-cover and sea-ice products, the albedo algorithm requires

several ancillary data sets including topography and landcover. A description of each step in the algorithm follows, including the inputs used in the MAS protoype as well as those currently proposed for the production MODIS version of the algorithm.

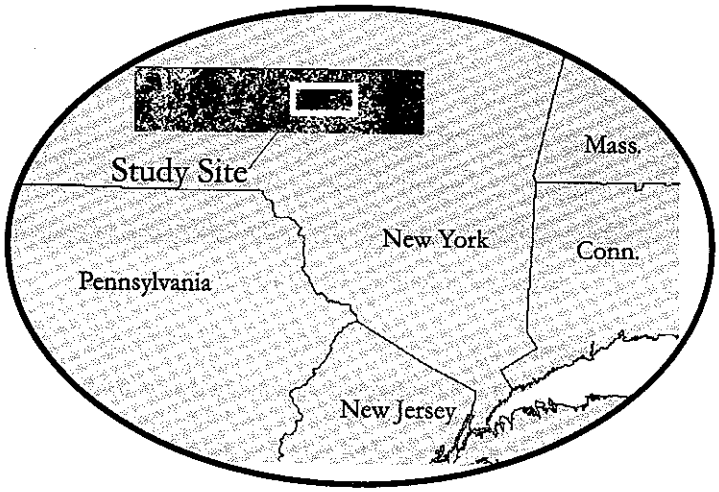


Figure 3: Study area used in developing the preliminary MODIS snow albedo algorithm.

**1) Determination of presence or absence of clouds and snow**

The snow albedo algorithm will only be applied to pixels that have been identified as cloud-free by the MODIS cloud mask (MOD 35) and as snow-covered by the snow-cover algorithm (MOD10). The MODIS cloud mask presents four different probabilities (cloudy, probably clear, confident clear and high confident clear) of a pixel being cloud-free. Currently, if there is any chance of a pixel being cloud-free, the snow-cover algorithm attempts to detect snow. It is feasible that the snow-cover algorithm will be able to operate over a wider range of cloud conditions than the albedo algorithm and the albedo algorithm may need to be restricted to conditions where the cloud mask predicts a higher probability of the pixel being cloud-free. In the prototype algorithm, the MAS versions of the cloud detection algorithm and MAS snow-cover algorithm are used to supply the necessary inputs. Field observations showed the area to be nearly cloud-free and essentially 100% snow-covered during image acquisition.

**2) Determination of atmospherically-corrected surface reflectance**

As stated above, primary inputs into the MODIS snow albedo algorithm are the atmospherically-corrected MODIS surface reflectances (the MOD09 product). Despite limitations in the atmospheric correction algorithm over snow-covered surfaces, it is unfeasible to perform a separate atmospheric correction solely for the snow albedo product. While MAS prototyping efforts will use a modified version of S6 (Vermote *et al.*, 1997), atmospheric corrections have not been applied to the images presented here because for this area adequate ground measurements were not taken to validate albedo retrievals.

In the algorithm prototyping efforts, five of the seven MODIS land bands (1, 2, 4, 6, and 7) have MAS equivalents (2, 7, 1, 10, and 20) that can be used in the prototyping efforts. The radiance values of these five MAS bands were first converted to reflectances (Gumley *et al.*, 1994). They were then projected into a Universal Transverse Mercator (UTM) projection with 50 meter spatial resolution using the latitudes/longitudes provided for each MAS pixel and with nearest-neighbor resampling. Unfortunately, these latitudes and longitudes are based on aircraft position, and can be off more than a kilometer. A ground control warp, again using nearest-neighbor resampling, was then required to coregister the MAS images with the other input data sets (**Figure 4**).

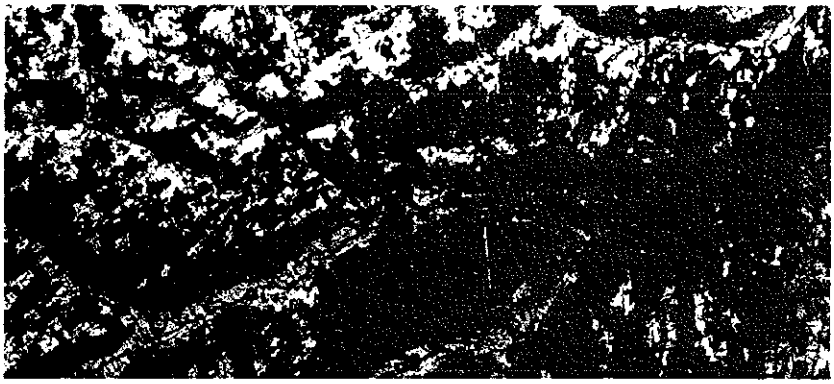

Figure 4: Uncorrected MAS image (band 1)

### 3) Correction for slope effects

As snow cover is prevalent in mountainous areas, correction of the surface reflectance for topography is necessary (e.g. Proy *et al.*, 1989). Currently, the algorithm corrects for the orientation of the surface relative to the sun, but ignores effects of radiation reflected from and shadows cast by adjacent topography. These additional corrections may be incorporated into future versions.

For MODIS, the Global 30 Arcsecond (GTOPO30) digital elevation model (DEM) available from the United States Geological Survey (USGS) will be used for the topographic corrections. The resolution of GTOPO30 is approximately 1 km. This necessitates producing the snow albedo product at 1 km as opposed to the 500 m of the snow cover products. From the DEM, the slope and aspect of each pixel is determined using the best-fit plane to all elevations in the surrounding 3 x 3 pixel window.

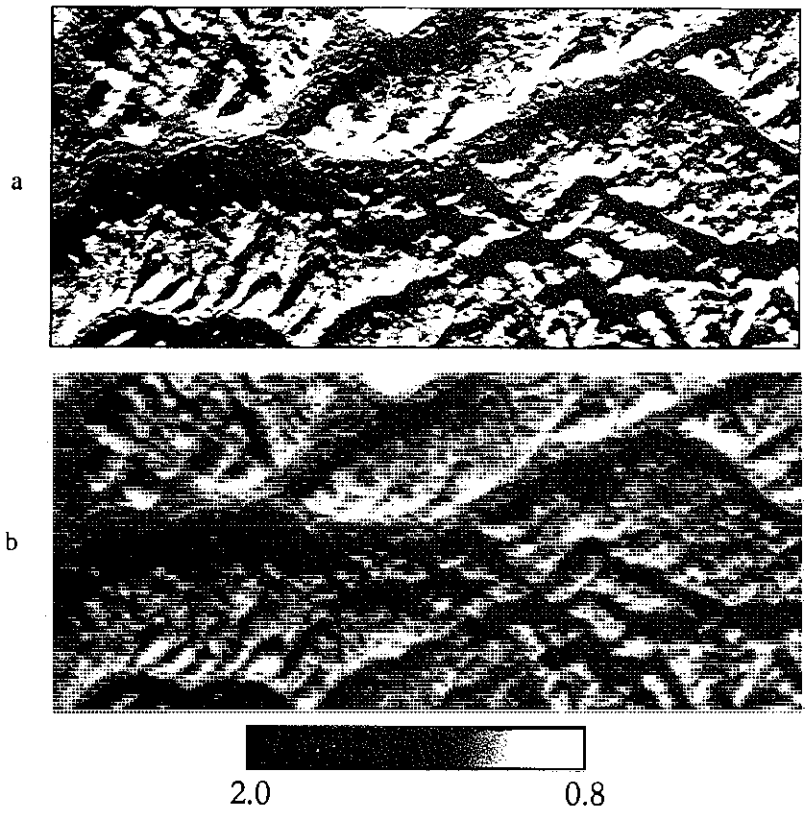


Figure 5: (a) Hillshade map of the DEM for the area (b) Topographic correction factor. Note the colors have been flipped (black representing high values) to correspond more closely to the hillshade image.

The much higher resolution of the MAS, requires a finer resolution DEM for use in the prototype and 30 m DEMS available from the USGS are used. All available 7.5 minute quadrangles covering the study area were merged and resampled to the 50 meter resolution of the MAS (**Figure 5a**). The slope and aspect of each 50 m pixel was then determined.

Given the slope ($\theta_s$) and aspect ($\phi_s$) of a pixel as well as the solar zenith ($\theta_0$) and azimuth ($\phi_0$), it is possible to develop a terrain correction factor (cf) that is used to normalize the amount of radiation received on the slope to that received on a horizontal surface:

$$cf = \frac{1}{\cos\Theta / \cos\theta_0} \tag{5}$$

Where $\cos\Theta = \cos\theta_s \cos\theta_0 + \sin\theta_s \sin\theta_0 \cos(\phi_0 - \phi_s)$. The topographic correction factor (cf) for each pixel is shown in **Figure 5b**.

**4) Determination of vegetation type**

In order to determine whether an isotropic or forward scattering BRDF model should be used to adjust the topographically-corrected surface reflectances, it is necessary to determine if the surface is forested or non-forested. Unfortunately, the BRDF of snow-covered forests is unknown so no adjustment can be made. However, for non-forested areas a snow BRDF model will be used to adjust the reflectances. Initially, the algorithm will utilize the 1 km Global Landcover Characterization Database available from the USGS EROS data center, but eventually will use the MODIS Landcover/Landcover Change product (MOD 12) to determine whether or not a pixel is forested. Unfortunately, these continental scale datasets are unsuitable for use with the higher resolution MAS imagery so in the prototype version the snow BRDF adjustment has been applied to all pixels regardless of cover type. In future versions of the prototype algorithm, 1:250,000 landcover information will be used to discriminate between forests and non-forested areas.

**5) Correction for anisotropy in snow reflectance**

In order to derive an albedo measurement from a satellite observation which is made at a specific time and with a specific view azimuth and zenith angle, knowledge of the BRDF of the snow surface is necessary. Ideally, a model of snow BRDF would be developed from a large number of field observations made under a wide range of solar zenith angles, atmospheric and snowpack conditions. Unfortunately, the dearth of BRDF measurements made for snow and ice currently precludes this approach.

Recently, several investigators (Fily *et al.*, 1997; Nolin and Stroeve, 1997; Stroeve *et al.*, 1997) have demonstrated the potential for using a discrete-ordinate radiative transfer model (Stamnes *et al.*, 1988) to model snow BRDF. This model is appropriate for modeling multiple scattering in particulate media and calculates the angular distribution of reflected radiation. The optical properties needed for the Disort model include snowpack optical thickness, single scattering albedo, an asymmetry parameter (or a description of the scattering phase function). Fortunately, the required parameters can be calculated from Mie theory and the refractive indices for ice using the physical properties of the snowpack, depth, bulk density and equivalent grain size.

A series of snow BRDF models, representing a suite of solar zenith angles and varying ratios of diffuse to direct beam radiation, have been generated for the center wavelength of each MODIS and MAS band. In all cases an optically-equivalent grain size of 250 μm was used. While, the modeled BRDF appear to be reasonable in the visible and near-IR portions of the spectrum, they appear suspect in the shortwave IR (1.6 and 2.1 μm bands) so a different approach may be necessary at these wavelengths (**Figure 6**). While the modeled BRDF appear reasonable, comparisons with measured BRDF (e.g.Leshkevich *et al.*, 1990) will be part of future algorithm validation efforts.

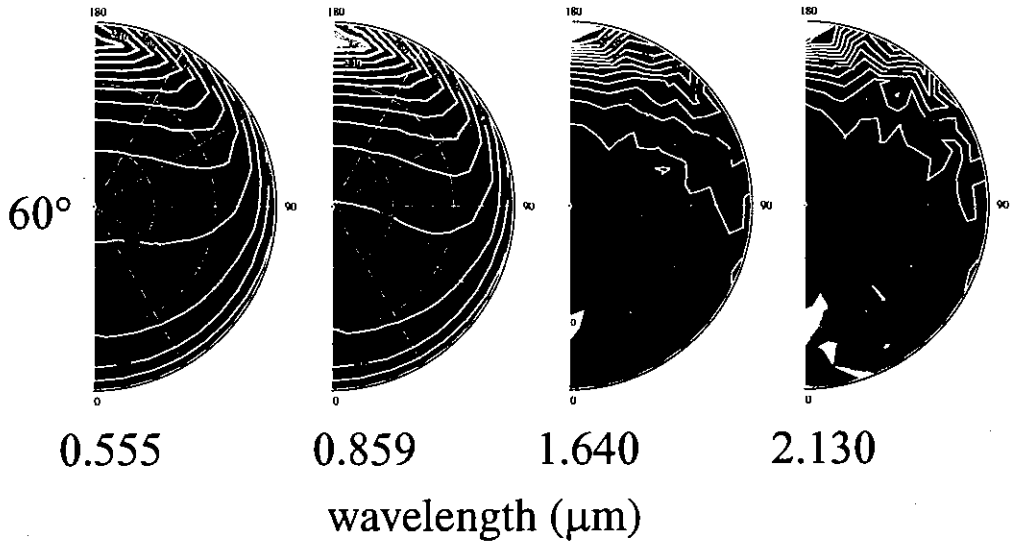


Figure 6: Anisotropic response function at four wavelengths for a 60° solar zenith angle

**6) Perform a narrow-to-broadband conversion**

Building upon similar efforts for MODIS (Liang *et al.*, 1998), weighting coefficients to convert the MAS spectral reflectances to broadband albedos in the visible (0.4-0.7 μm), near-IR (0.7-5.0 μm), and shortwave (0.4-5.0 μm) are being developed.

## CONCLUSIONS AND FUTURE RESEARCH DIRECTIONS

Because the snow and sea ice albedo algorithm is a work in progress, few concrete conclusions can be made. However, based on these preliminary MAS prototyping efforts, development of a MODIS snow and sea-ice albedo algorithm using existing MAS data appears to be feasible. A spectral albedo image for a single visible MAS band is shown in **Figure 7**. Comparison of the albedo image with the corresponding uncorrected MAS reflectance image (**Figure 4**) illustrates the influence of the topographic correction which appears to successfully remove most of topographically induced reflectance variations seen in the original image. However, the albedo image is quite visibly striped. The striping is due to subtle errors in the DEM which are amplified in the derivative slope and aspect maps. This is expected and highlights the potential problems and uncertainties that will exist in the MODIS snow albedo algorithm, simply because of the errors inherited from the various inputs.

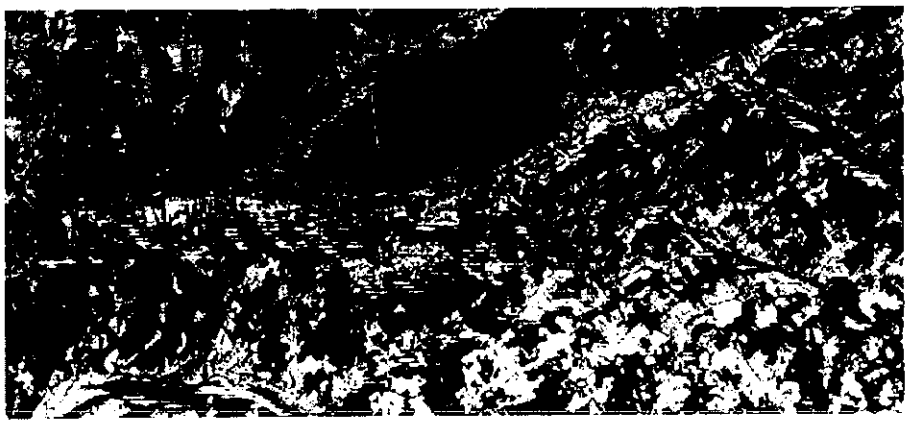

Figure 7: Preliminary snow albedo image for MAS band 1

Future algorithm development efforts will focus on atmospheric correction of MODIS imagery and improvement of the correction for the forward-scattering nature of snow reflectance

in the algorithm. Multiple MAS images were collected over Madison, Wisconsin, during January and February of 1997 under varied atmospheric conditions and will be used to assess the performance of the algorithm under a wide range of atmospheric and cloudiness conditions. The repeatability of albedo retrievals will be tested using a flat site, Lake Mendota, where snow conditions were monitored during the missions.

## ACKNOWLEDGEMENTS

The MODIS snow albedo work has benefited greatly from discussions with Anne Nolin of the National Snow and Ice Data Center and Jiancheng Shi of University of California-Santa Barbara. This work was carried out under NASA contract NAG5-8137.

## BIBLIOGRAPHY

De Abreau, R. A., Key, J., Maslanik, J. A., Serreze, M. C., and LeDrew, E. F. (1994). Comparison of in situ and AVHRR-derived broadband albedo over Arctic sea ice. *Arctic* **147,** 288-29?

Fily, M., Bourdelles, B., Dedieu, J. P., and Sergent, C. (1997). Comparison of *In Situ* and Landsat Thematic Mapper derived snow grain characteristics in the Alps. *Remote Sensing of Environment* **59,** 452-460.

Foster, J. L., and Chang, A. T. C. (1993). Snow Cover. *In* "Atlas of Satellite Observations Related to Global Change." (R. L. Burney, C. L. Parkinson, and J. L. Foster, Eds.), pp. 361-370. Cambridge University Press, Cambridge.

Gumley, L., Hubanks, P., and Masuoka, E. (1994). MODIS Airborne Simulator Level-1B Users Guide.

Hall, D. K., Riggs, G., A., and Salomonson, V. V. (1995). Development of methods for mapping global snow cover using moderate resolution imaging spectroradiometer data. *Remote Sensing of Environment* **54,** 127-140.

Knap, W. H. (1997). "Satellite-derived and ground-based measurements of the surface albedo of glaciers.".

Knap, W. H., and Oerlemans, J. (1996). The surface albedo of the Greenland ice sheet: satellite-derived and in situ measurements in the Søndre Strømfjord area during the 1991 melt season. *Journal of Glaciology* **42,** 364-374.

Leshkevich, G. A., Deering, D. W., Eck, T. F., and Ahmad, S. P. (1990). Diurnal patterns of the bi-directional reflectance of fresh-water ice. *Annals of Glaciology* **14,** 153-157.

Liang, S., Strahler, A., and Walthall, C. (1998). Retrevial of Land Surface Albedo from Satellite Observations: A Simulation Study. *In* "Geoscience and Remote Sensing Symposium (IGARSS '98).", pp. 1286-1288. IEEE International.

Nolin, A. W., and Stroeve, J. (1997). The changing albedo of the Greenland Ice Sheet: implications for climate change. *Annals of Glaciology* **25,** 51-57.

Proy, C., Tanré, D., and Deschamps, P. Y. (1989). Evaluation of topographic effects in remotely sensed data. *Remote Sensing of Environment* **30,** 21-32.

Schweiger, A. J., Serreze, M. C., and Key, J. R. (1993). Arctic sea ice albedo: a comparison of two satellite-derived data sets. *Geophysical Research Letter* **20,** 41-44.

Stamnes, K., Tsay, S., Wiscombe, W., and Jayaweera, K. (1988). Numerically stable algorithm for discrete-ordinate-method radiative transfer in multiple scattering ane emitting layered media. *Applied Optics* **23,** 2502-2509.

Steffen, K. (1996). Effect of solar zenith angle on snow anisotropic reflectance. *In* "IRS'96: Current Problems in Atmospheric Radiation." (Smith, and Stamnes, Eds.), pp. 41-44.

Stroeve, J., Nolin, A., and Steffen, K. (1997). Comparison of AVHRR-derived and in situ surface albedo over the Greenland Ice Sheet. *Remote Sensing of Environment* **62,** 262-276.

Vermote, E. F., Tanré, D., Deuze, J. L., Herman, M., and Morcrette, J. J. (1997). Second simulation of the satellite signal in the solar spectrum: an overview. *IEEE Transactions on Geoscience and Remote Sensing* **35,** 675-686.

Vermote, E. F., and Vermeulen, A. (1999). "Atmospheric correction algorithm: spectral reflectances (MOD09)." MODIS Algorithm Theoretical Basis Document

Warren, S. G. (1982). Optical properties of snow. *Reviews of geophysics and space physics* **20,** 67-89.